

# PHOTOPRODUCTION OF MUON PAIRS IN CARBON

A. Alberigi-Quaranta, M. De Pretis, G. Marini, A. Odian<sup>(\*)</sup>, G. Stoppini and L. Tau

Laboratori Nazionali di Frascati, Roma

(presented by A. Odian)

In the past few years, the discovery of a new interaction of the  $\mu$  meson has been the frustrated aim of several experimentalists. Recently a group<sup>1)</sup> at CERN, by means of a classical experiment on the muon magnetic moment, once again failed to reveal anomalies, thereby strongly supporting the complete equivalence between electrons and muons. We

furnish here new evidence for this, by reporting on an experiment in which the absolute cross-section for muon pairs photoproduced in carbon has been measured, in a region of low momentum transfer to the nucleus (40-80 MeV/c).

A drawing of the experimental apparatus is shown in Fig. 1. The 1000 MeV bremsstrahlung beam of the

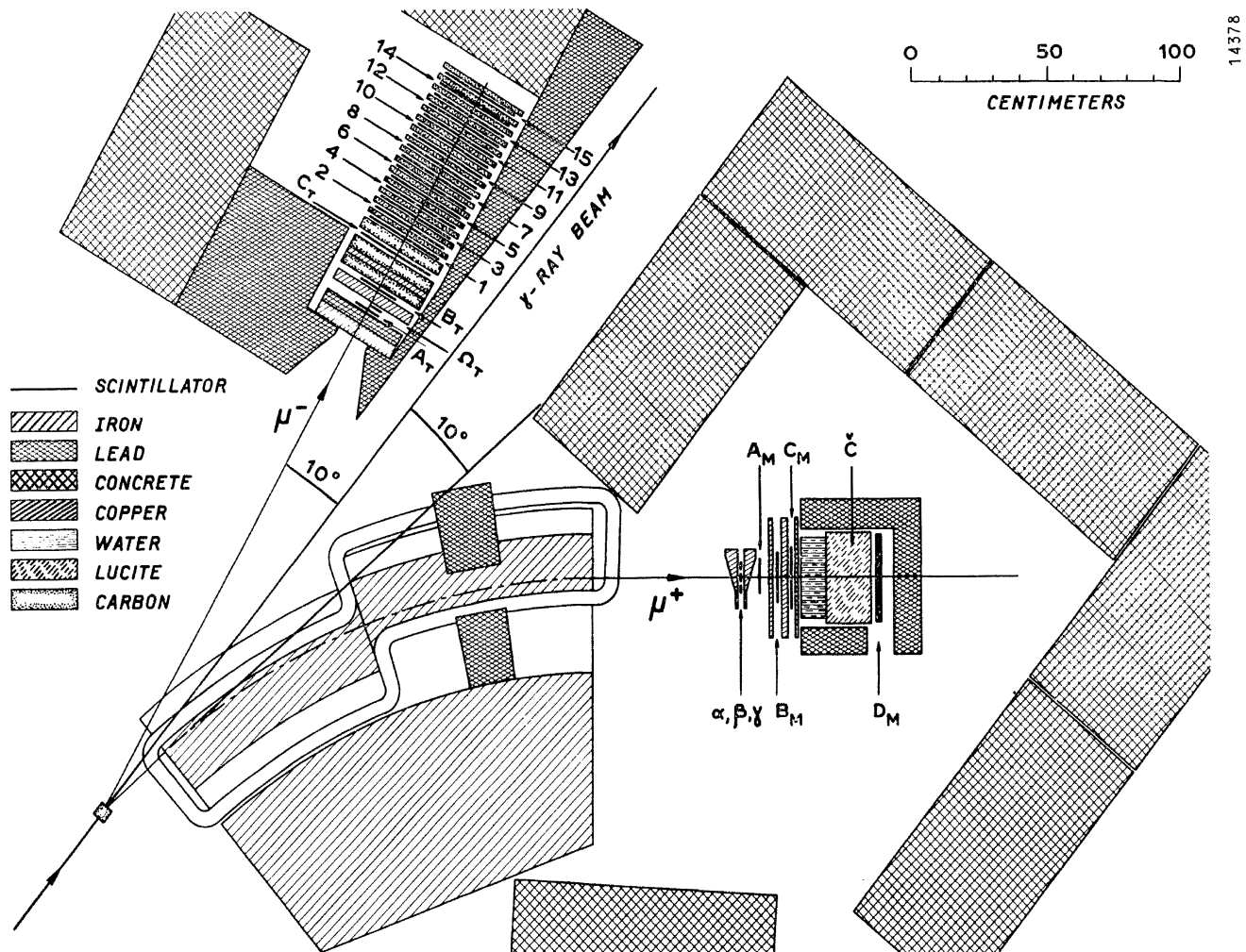


Fig. 1 A drawing of the experimental apparatus.

(\*) On leave of absence from the University of Illinois, Urbana, Ill.

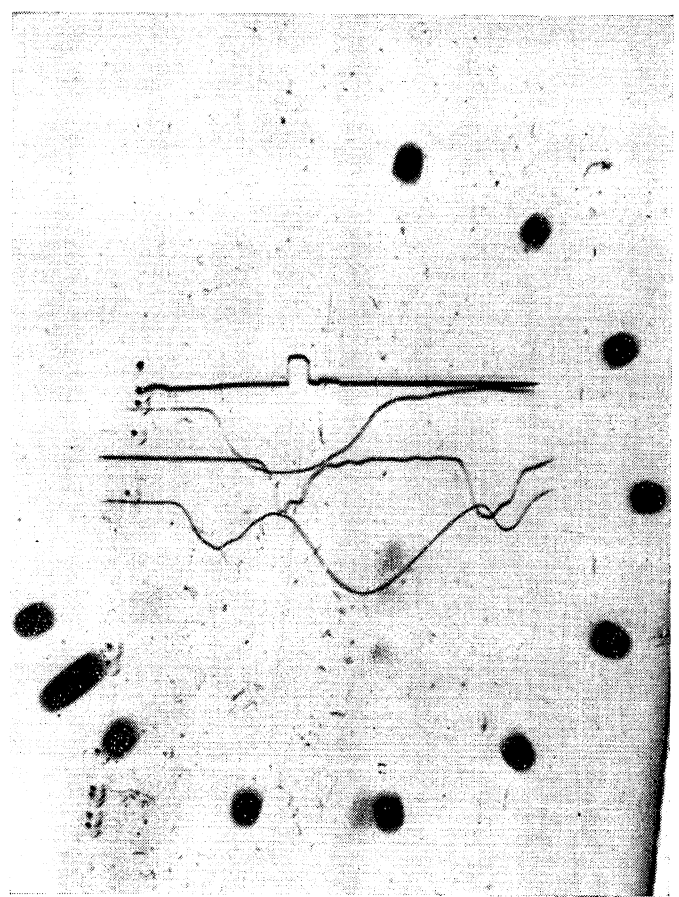
Frascati Electrosynchrotron was collimated to a 2 cm diameter spot on a carbon target of 5 cm in length ( $8.8 \text{ g/cm}^2$ ). Positive muons emitted at  $10^\circ$  in the momentum interval from roughly 300 to 400 MeV/c were first deflected by a double focusing magnetic spectrometer <sup>2)</sup> to traverse one of three momentum defining scintillation counters  $\alpha$ ,  $\beta$  and  $\gamma$ . The muons then produced a four-fold coincidence in scintillators  $A_M B_M C_M$  and  $D_M$ , and gave Čerenkov light in the water+lucent counter  $\check{C}$ . Pions, on the contrary, were slowed down to about the Čerenkov threshold by copper absorbers. However, for this method of separation to be effective, the spectrometer should accept a small momentum interval, which, in turn, would produce a low counting rate. To avoid this, two appropriately shaped copper wedges were placed at the focal plane of the magnet to monocromatize the particles. Counters  $A_M B_M$  and  $C_M$  were 1 cm thick, while  $D_M$ , which was used also in pulse height analysis, was 3 cm thick.

At  $10^\circ$  on the opposite side of the photon beam, a range telescope of 19 counters detected the negative muons. These were required to traverse at least the four counters  $A_T B_T C_T$  1 and to be in coincidence with the positive muons on the magnet side. The first counter  $A_T$ , which defined the solid angle, was followed by the counter  $\Omega_T$  which was half as wide, so as to give a reasonably large angular acceptance without loss in angular resolution. Spaced between these five counters a thick absorber reduced the electron and pion background. To reduce this background still further, use is to be made of the remaining portion of the telescope, made up of 14 scintillators measuring  $30 \times 30 \times 1 \text{ cm}$ , and separated by carbon layers of 2.3 cm in thickness ( $4.9 \text{ g/cm}^2$ ). Whenever a coincidence occurred between the outputs of  $(A_M, B_M, C_M, D_M)$  and  $(A_T, B_T, C_T, 1)$ , two hodoscopes of 14 indicator lights each were activated. Both hodoscopes were connected with the 14 counters in such a way that the first showed the counters traversed by the incoming muon, and the second those traversed by the muon decay electron, thus allowing us to verify that the electron originated at the end point of the muon.

All the information necessary to identify each event was recorded on a four-trace oscilloscope, triggered by the master eight-fold coincidence. On the first trace, which had a slow sweep speed, a pulse from the electron gave the time interval between the muon arrival

and its decay, thus allowing us to verify its correct exponential time distribution. The other three traces had high sweep speeds. On the second we displayed pulses from counters  $\alpha$ ,  $\beta$  and  $\gamma$ , which determined the  $\mu^+$  momentum. On the third a pulse from  $C_T$  and a pulse from  $C_M$  permitted us to establish the coincidence between the two muons with a much higher resolving time than with electronic circuits and allowed a simultaneous measure of the background of accidentals. Finally, on the fourth trace we displayed pulses from  $D_M \check{C}$  and  $\Omega_T$ . Fig. 2 shows a photograph of a good event and Fig. 3 the block diagram of the electronics.

Owing to loss of muons by scattering out of the telescope, a complete analysis of our data must include a Monte Carlo calculation of our detection efficiency. This is under way, and we present in this note only an alternative analysis in which results from the hodoscopes are not taken into account. Our present procedure is therefore equivalent to integrating



14381

**Fig. 2** Photogram of a good event, in which the  $\mu^-$  stopped between counters 11 and 12 and the decay electron was emitted backwards (the spots are from the lights of the two hodoscopes).

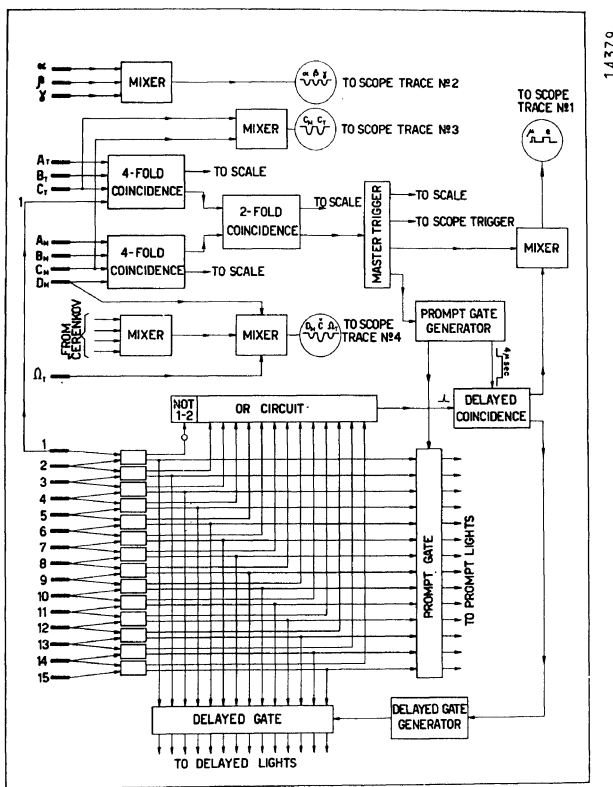


Fig. 3 Block diagram of the electronics. It includes a system of 14 double coincidences (obtained by letting each counter in the telescope make a coincidence with the next) connected to the muon hodoscope and the electron hodoscope through a prompt gate and a delayed gate.

over the  $\mu^-$  energy from the 458 MeV minimum required to trigger the four counters to the maximum imposed by the conservation of energy.

Fig. 4 shows the distribution of the time intervals separating the pulses  $C_T$  and  $C_M$ . Its sharp peak, due to pairs of particles produced in a single elementary act, rises above a background of accidentals showing the expected effect of bunching produced by the synchrotron radio-frequency. After subtracting this background, we must correct our data for pairs of pions (plus their decay muons) and for pairs of electrons. To this end, we compared the combined  $\check{C}$  and  $D_M$  pulse height distribution of our events with the corresponding distributions for electrons and pions. The distribution for the latter was taken with the magnet located at  $30^\circ$ , where counts from electrons or electromagnetic muons are negligible, and the distribution for electrons was taken at  $10^\circ$  with a lead converter increasing the number of electrons in the primary beam. Roughly speaking, pions plus their decay muons give a broad spectrum in  $\check{C}$ , while electrons give a broad spectrum in  $D_M$ ;

on the contrary, the distribution for electromagnetic muons, obtained at  $30^\circ$  by simulating them with pions of appropriate momentum, shows well defined peaks in both these counters (see Fig. 5). More precisely, we divided our events into three groups: (1) events with  $D_M$  pulse height smaller than 4 mm, (2) events with  $D_M$  at least 4 mm but  $\check{C}$  smaller than 4 mm, (3) events with both  $D_M$  and  $\check{C}$  at least 4 mm, and could show that 98.4% of the electromagnetic muons are in this last group. In it we had 1695 events, collected at a rate of about one every 6 minutes. From the other two groups we find that 42 of these events are electrons and 252 are pions plus decay muons.

TABLE I

Ratios of the experimental to the theoretical cross-sections for the three momentum channels of the  $\mu^+$  and for the two angular channels of the  $\mu^-$

$\bar{p}_M$	329	360	393 MeV/c
$\bar{\theta}_T$			
9.3°	$0.88 \pm 0.13$	$0.90 \pm 0.09$	$1.04 \pm 0.10$
10.7°	$0.99 \pm 0.15$	$1.15 \pm 0.10$	$1.11 \pm 0.10$

Table I shows our results, in the form of ratios of the absolute experimental cross-sections to the theoretical. To obtain the latter, the Bethe-Heitler<sup>3)</sup> proton cross-sections were first corrected for the

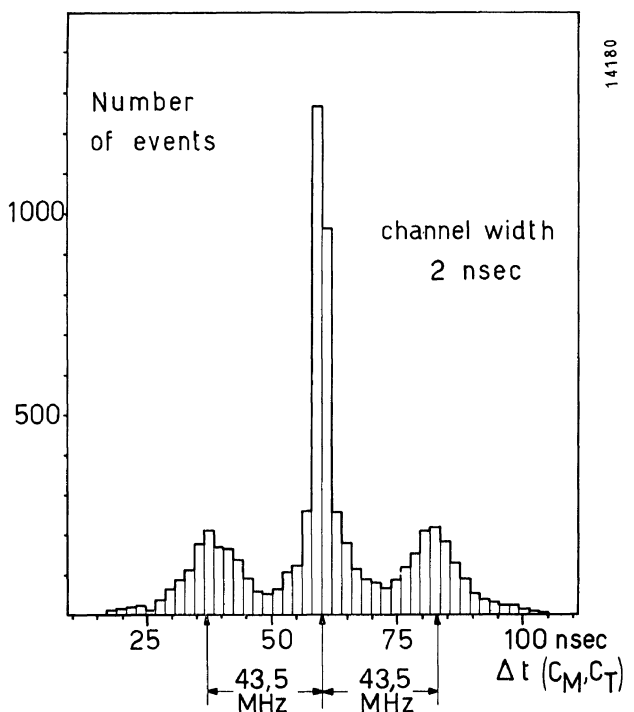


Fig. 4 Timing between pulses from  $C_T$  and  $C_M$ . The value 43.5 MHz is that of the synchrotron radio-frequency.

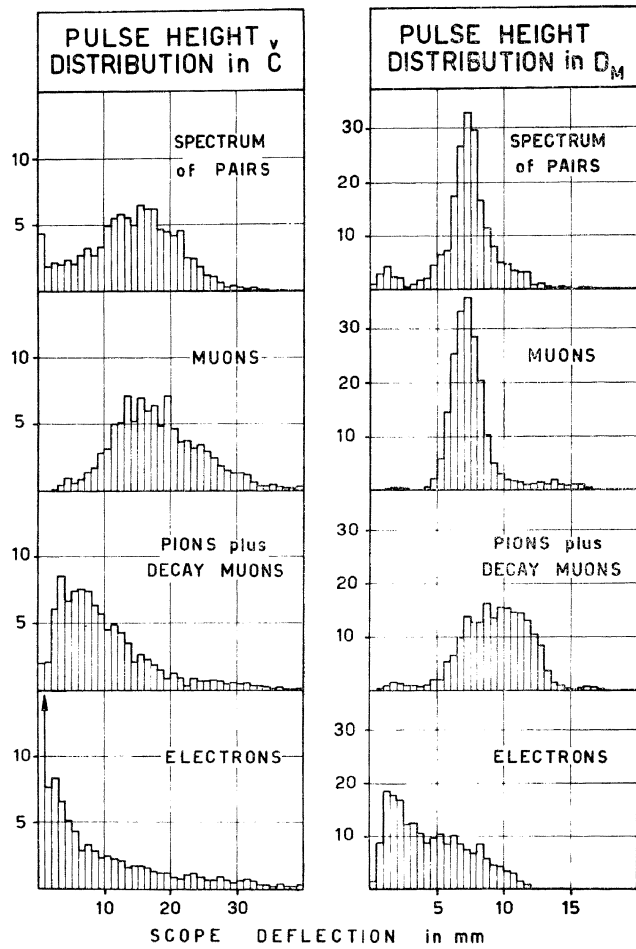


Fig. 5 Pulse height distributions in  $D_M$  and  $C$  obtained under different experimental conditions as explained in the text.

carbon form factors <sup>4)</sup> and for inelastic processes according to the formula <sup>(\*)</sup>  $\sigma_C = \sigma_{BH}(Z^2 F^2 + Z(1 - F^2))$ . They were then integrated over the  $\mu^+$  and  $\mu^-$  solid

angles and over the bremsstrahlung spectrum. Folded into the integrals were the resolution curves of the spectrometer, as obtained by extrapolating  $\alpha$  particle calibration measurements <sup>2)</sup> to our well-below-saturation field setting. Not included in the calculation were radiative corrections (estimated by Bjorken et al. <sup>5)</sup> to be less than 1.5%) and nuclear recoil effects. The errors quoted in the table are statistical: we estimate other uncertainties in the experimental cross-sections (coming mainly from the beam calibration and the bremsstrahlung spectrum) to be less than 2%.

Differences from unity in the six ratios shown are hardly significant: the overall average gives  $1.00 \pm 0.05$ . Assuming this error, and taking into account the range of variation of the four-momentum transfer  $q$  to the virtual muon (135-185 MeV/c), we conclude that no anomalous behaviour is observed, within 5% accuracy, down to a distance  $\hbar/q = 1.2 \times 10^{-13}$  cm. For those who believe in cut-off theories, we may, of course, push this value further, and set, with 95% confidence, a limit of  $2 \times 10^{-14}$  cm for a cut-off in the virtual muon propagator <sup>6)</sup>. Accordingly, we confirm the well known result <sup>1)</sup> obtained at CERN. Finally, the total energy of the two muons in their centre of mass ranged from 240 to 290 MeV, and we exclude from this interval muon-muon interaction effects larger than 5%. Effects due to possible leptonic decays of the  $\omega^0$  and  $\eta^0$  particles <sup>7)</sup>, or to the  $\sigma^0$  meson conjectured by Schwinger <sup>8)</sup>, may be observed at higher energies. We are planning an experiment to explore these higher masses, and ranges of higher momentum transfer.

#### LIST OF REFERENCES

1. G. Charpak, F. Farley, R. Garwin, J. Sens, V. Telegdi and A. Zichichi: Phys. Rev. Letters 6, 128 (1961).
2. G. Sacerdoti and L. Tau (to be published in Nucl. Instr. and Meth.).
3. W. Heitler: Quantum Theory of Radiation (Oxford, 1954) third edition, p. 257.
4. R. Hofstadter: Ann. Rev. of Nucl. Sci. 7, 231 (1957). Our momentum transfer to the carbon nucleus ranged from 40 to 80 MeV/c, thus  $F^2$  from 0.93 to 0.76.
5. J. D. Bjorken, S. D. Drell and S. C. Frautschi: Phys. Rev. 112, 1409 (1958).
6. J. D. Bjorken and S. D. Drell: Phys. Rev. 114, 1368 (1959); S. D. Drell, Ann. of Phys. 4, 75 (1958). Criticisms of cutoff theories are found also in R. Feynman, Theory of Fundamental Processes, New York, 1961, p. 145.
7. Y. Nambu and J. J. Sakurai: Phys. Rev. Letters 8, 79 (1962).
8. J. Schwinger: Ann. of Phys. 2, 407 (1957).

(\*) Inelastic corrections given by the second term are of the order of 3%.

## DISCUSSION

PANOFSKY: When you said you had only 10% to subtract for pion contamination, is that mainly due to pions which decay in flight in both channels so that they look like muons?

ODIAN: We shall eliminate this contamination using the information on the  $\mu^-$  decay from the range telescope. To do this we need a Monte Carlo calculation for the detection efficiency.

SCHIFF: The "Z" term in the formula that you quote in the abstract for the modified Bethe-Heitler formula assumes a sum rule which arises from a sum over all excited and dissociated states of the carbon nucleus. Did you make an estimate of the error involved in that assumption and could it be of the order of the experimental error?

ODIAN: That term is about 2% of the total, and cannot modify things very much. It is within our experimental error.

## HYPERFINE STRUCTURE OF MUONIUM

J. Bailey, W. Cleland, V. W. Hughes, R. Prepost, and K. Ziock

Yale University, New Haven, Conn.

(presented by V. W. Hughes)

A precision measurement of the hyperfine structure splitting,  $\Delta v$ , of muonium ( $\mu^+e^-$ ) in its ground  $1^2S_{1/2}$  state has been made by a special microwave spectroscopy technique.<sup>1)</sup>

If the muon is a particle which obeys the modern Dirac theory and which differs from the electron only

in its mass value, then the hfs of muonium can be calculated from the quantum electrodynamic theory of the muon, electron, and photon fields. The result can be expressed as a power series in the small parameters  $\alpha$  and  $(m_e/m_\mu)$ , and (to terms of order  $\alpha^2$  and  $\alpha(m_e/m_\mu)$ ) is given by<sup>1)</sup>

$$\Delta v_{(\text{theor})} = \left( \frac{16}{3} \alpha^2 c R_\infty \frac{\mu_\mu}{\mu_0} \right) \left( 1 + \frac{m_e}{m_\mu} \right)^{-3} \left( 1 + \frac{3}{2} \alpha^2 \right) \left( 1 + \frac{\alpha}{2\pi} - 0.328 \frac{\alpha^2}{\pi^2} \right) \left( 1 + \frac{\alpha}{2\pi} + 0.75 \frac{\alpha^2}{\pi^2} \right) (1 - 1.81 \alpha^2) \left( 1 - \frac{3\alpha}{\pi} \frac{m_e}{m_\mu} \ln \frac{m_\mu}{m_e} \right) \quad (1)$$

in which  $\alpha$  = fine structure constant,  $c$  = velocity of light,  $R_\infty$  = Rydberg constant for infinite mass,  $\mu_\mu$  = muon magneton ( $e\hbar/2m_\mu c$ ),  $\mu_0$  = electron Bohr magneton,  $m_e$  = electron mass, and  $m_\mu$  = muon mass. The first bracketed factor is the Fermi value for the hfs; the second factor is a reduced mass correction;

the third factor is the Breit relativistic correction; the fourth and fifth factors are the  $g/2$  values for the electron and the muon; the sixth factor is a second order radiative correction; the seventh factor is a relativistic recoil factor. Use of the best modern values of the fundamental atomic constants gives:

$$\Delta v_{(\text{theor})} = 4463.13 \pm 0.10 \text{ Mc/sec.}$$

In computing this value we have used

$$(m_\mu/m_e) = (206.76 \pm 0.02), \alpha^{-1} = 137.0391 \pm 0.0006,$$

and

$$\frac{\mu_\mu}{\mu_0} = \left( \frac{\mu'_\mu}{\mu_p} \right) \left( \frac{\mu_p}{\mu'_e} \right) \left( 1 + \frac{\alpha}{2\pi} - 0.328 \frac{\alpha^2}{\pi^2} \right) / \left( 1 + \frac{\alpha}{2\pi} + 0.75 \frac{\alpha^2}{\pi^2} \right),$$